Probing the Mechanistic and Energetic Basis for the Weak-Link Approach to Supramolecular Coordination Complexes

Bradley J. Holliday, You-Moon Jeon, Chad A. Mirkin,* and Charlotte L. Stern

Department of Chemistry and Center for Nanofabrication and Molecular Self-Assembly, 2145 Sheridan Road, Northwestern University, Evanston, Illinois 60208-3113

Christopher D. Incarvito, Lev N. Zakharov, Roger D. Sommer, and Arnold L. Rheingold

Department of Chemistry and Biochemistry, University of Delaware, Newark, Delaware 19716

Received September 6, 2002

Through the Weak-Link Synthetic Approach, the unsymmetric hemilabile ligand, 1,4-bis-(2-diphenylphosphinoethoxy)naphthalene (**7**), has been used to prepare binuclear Rh(I) macrocycles in a two-step fashion. The intermediate structure, [(μ^2,η^1:η^4:η^1-(1,4-bis(2-(diphenylphosphino)ethoxy)naphthalene))$_2$Rh$_2$][BF$_4$]$_2$ (**8**), and several macrocyclic complexes, [(μ^2-1,4-bis(2-(diphenylphosphino)ethoxy)naphthalene)$_2$Rh$_2$(CH$_3$CN)$_4$][BF$_4$]$_2$ (**9**), [(μ^2-1,4-bis-(2-(diphenylphosphino)ethoxy)naphthalene)$_2$Rh$_2$(CO)$_6$][BF$_4$]$_2$ (**10**), and [(μ^2-1,4-bis(2-(diphenylphosphino)ethoxy)naphthalene)$_2$(CO)$_2$Rh$_2$(CH$_3$CN)$_2$][BF$_4$]$_2$ (**11**), are reported herein. Additionally, the mononuclear Rh(I) complexes, [(η^1:η^4:η^1-1,4-bis(2-(diphenylphosphino)ethoxy)-naphthalene)Rh][BF$_4$] (**12**) and [(η^1:η^1-1,4-bis(2-(diphenylphosphino)ethoxy)naphthalene)-(CO)Rh(CH$_3$CN)][BF$_4$] (**13**), were isolated and fully characterized. Single-crystal X-ray diffraction structures of **8**, **9** (*cis*-, *anti*-), **11**, and **12** were determined. 2-D solution NMR studies and the solid-state crystal structures of **8** and **12** suggest that the arenes bind to Rh(I) in predominantly an η^4-fashion. The conversion of dimer **8** into monomer **12** was monitored under a variety of conditions. The kinetic investigation of this process as a function of temperature with a series of phosphine-based ligands present has afforded the thermochemical parameters of this conversion, which are consistent with an associative mechanism. Significantly, this work represents the first study aimed at gaining mechanistic insight into the conversion of the binuclear intermediates into the mononuclear products formed in the Weak-Link Approach. The high activation barrier and associative nature of this step is what allows one to efficiently synthesize targeted macrocyclic and higher-ordered structures via the approach.

Introduction

The design and synthesis of inorganic and organometallic macrocycles with tailorable host−guest chemistry and catalytic properties have been the subject of intense research over the past decade.[1] Three general coordination chemistry-based synthetic approaches have been developed for preparing such structures: the Directional-Bonding, Symmetry-Interaction, and Weak-Link Approaches.[2] With these approaches one can construct a wide variety of architectures that vary in size, chemical complexity, and structural flexibility. Coordination chemistry is used in these approaches because of the large number of available and tailorable metal−ligand coordination modes and accessible metal−ligand bond strengths when compared with the covalent chemistry of carbon.

From a mechanistic standpoint, these three strategies can be broken into two general categories: those under thermodynamic control and those under kinetic control. All of them rely on the concept of thermally annealing the reactants to avoid potential oligomeric and polymeric byproducts, which are often the initial complexes formed. However, in the case of the Directional-Bonding and Symmetry-Interaction Approaches, the overall ther-

* To whom correspondence should be addressed. Fax: (847) 467-5123. E-mail: camirkin@chem.nwu.edu.

(1) (a) Lehn, J.-M. *Supramolecular Chemistry*; VCH: New York, 1995. (b) Vögtle, F. *Supramolecular Chemistry*; Wiley: Chichester, 1991. (c) Caulder, D. L.; Raymond, K. N. *J. Chem. Soc., Dalton Trans.* **1999**, 1185−1200. (d) MacGillivray, L. R.; Atwood, J. L. *Angew. Chem., Int. Ed.* **1999**, *38*, 1018−1033. (e) Lawrence, D. S.; Jiang, T.; Levett, M. *Chem. Rev.* **1995**, *95*, 2229−2260. (f) Hunter, C. A. *Angew. Chem., Int. Ed. Engl.* **1995**, *34*, 1079−1081. (g) Kuehl, C. J.; Kryschenko, Y. K.; Radhakrishnan, U.; Seidel, S. R.; Huang, S. D.; Stang, P. J. *Proc. Natl. Acad. Sci. U.S.A.* **2002**, *99*, 4932−4936. (h) Leininger, S.; Olenyuk, B.; Stang, P. J. *Chem. Rev.* **2000**, *100*, 853−908. (i) Leininger, S.; Fan, J.; Schmitz, M.; Stang, P. J. *Proc. Natl. Acad. Sci. U.S.A.* **2000**, *97*, 1380−1384. (j) Cotton, F. A.; Lin, C.; Murillo, C. A. *Acc. Chem. Res.* **2001**, *34*, 759−771. (k) Caulder, D. L.; Raymond, K. N. *Acc. Chem. Res.* **1999**, *32*, 975−982. (l) Fujita, M. *Struct. Bonding* **2000**, *96*, 177−201. (m) Fujita, M.; Umemoto, K.; Yoshizawa, M.; Fujita, N.; Kusukawa, T.; Biradha, K. *Chem. Commun.* **2001**, 509−518. (n) Balzani, V.; Credi, A.; Raymo, F. M.; Stoddart, J. F. *Angew. Chem., Int. Ed.* **2000**, *39*, 3348−3391.

(2) Holliday, B. J.; Mirkin, C. A. *Angew. Chem., Int. Ed.* **2001**, *40*, 2022−2043.

10.1021/om020739c CCC: $22.00
Publication on Web 11/20/2002

Scheme 1

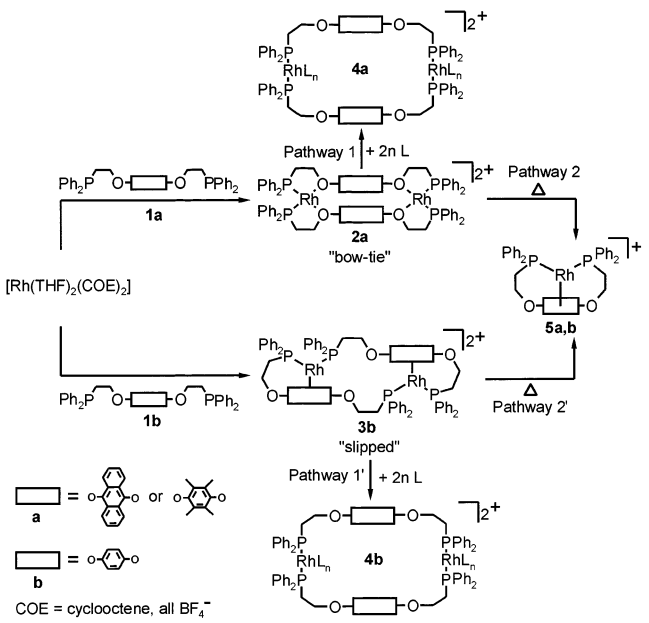

modynamic product, or global minimum on the reaction coordinate diagram, is the desired product of the reaction. Hence, reactions that rely on these approaches are referred to as being under thermodynamic control. In the case of the Weak-Link Approach, the desired product is a metastable intermediate structure, such as **2a** or **3b**, that is a local minimum on the reaction coordinate diagram with the mononuclear product, **5a**,**b**, being the ultimate thermodynamic sink of the reaction (Scheme 1). Through the careful selection of reaction conditions, the intermediates can be formed to the exclusion of both oligomeric and monomeric byproducts. Therefore, this approach is said to be under kinetic control. The binuclear kinetic intermediates in this reaction scheme can be reacted with small molecules, before they are converted to mononuclear complexes, to form the large ring structures that are typically the synthetic targets. While higher ordered and structurally dynamic architectures have been observed in all three approaches,[3] little mechanistic information is available regarding the possible pathways and the relative energetics of these conversions. The purpose of this paper is to examine a novel system relevant to the Weak-Link Approach in an attempt to understand the factors that control Pathways 1 and 2 (Scheme 1). Elucidating the reaction pathways is essential for fully understanding and utilizing this synthetic strategy.

Our group has extensively utilized the Weak-Link Approach to construct flexible binuclear macrocyclic and polynuclear three-dimensional cage architectures.[4−10] This approach relies on hemilabile ligands,[11] **1a**,**b**, to organize metal centers in the form of rigid condensed intermediates (**2a** and **3b**) with intentionally designed strong and weak metal links (Scheme 1). These structures can be subsequently opened into flexible macrocycles, **4a**,**b**, through high-yielding, small-molecule ligand substitution reactions which break the weak links but not the strong ones. For the systems studied thus far, two distinct structural isomers of the condensed intermediate, descriptively termed the "bow-tie" and "slipped" intermediates (**2a** and **3b**, respectively), have been characterized; they differ in the ligand-binding mode to the metal centers. Moreover, both isomers, under the appropriate conditions, often will convert to the thermodynamic mononuclear two-legged piano-stool complexes, **5a**,**b** (Scheme 1).[7]

In this paper we report the design and synthesis of a new naphthalene-based hemilabile ligand that allows us to systematically examine some of the important factors that control the formation of both condensed intermediates and the thermodynamic mononuclear products (Scheme 1). The motivation for synthesizing the naphthalene-based ligand **7** (Scheme 2) comes from the observed reaction pathways of the related ligand systems based on phenyl, biphenyl, anthracenyl, and duranyl moieties. In the case of Rh(I), when phenyl- or biphenyl-based phosphinoalkyl ether ligands were used, the slipped intermediates (binuclear Rh(I) structures that have two-legged piano-stool geometries with η^6-arenes and bis(phosphine)−Rh(I) bonds) are the predominant products.[7] However, when the duranyl- or anthracyl-based ligands were used, the bow-tie intermediates are the predominant products under virtually identical conditions.[4] As the intermediate structure between benzene and anthracene, we have studied the naphthalene-based ligand and its tendency to form either the bow-tie or slipped condensed intermediate. Importantly, since naphthalene groups undergo ring slippage more readily then single ring aromatic groups, binuclear intermediates formed from **7** undergo more

(3) (a) Schweiger, M.; Seidel, S. R.; Arif, A. M.; Stang, P. J. *Inorg. Chem.* **2002**, *41*, 2556−2559. (b) Campos-Fernández, C. S.; Clérac, R.; Koomen, J. M.; Russell, D. H.; Dunbar, K. R. *J. Am. Chem. Soc.* **2001**, *123*, 773−774. (c) Albrecht, M.; Napp, M.; Schneider, M.; Weis, P.; Fröhlich, R. *Chem. Commun.* **2001**, 409−410. (d) Beissel, T.; Powers, R. E.; Parac, T. N.; Raymond, K. N. *J. Am. Chem. Soc.* **1999**, *121*, 4200−4206. (e) Chi, X.; Guerin, A. J.; Haycock, R. A.; Hunter, C. A.; Sarson, L. D. *Chem. Commun.* **1995**, 2563−2565. (f) Fuss, M.; Siehl, H.-U.; Olenyuk, B.; Stang, P. J. *Organometallics* **1999**, *18*, 758−769. (g) Hiraoka, S.; Fujita, M. *J. Am. Chem. Soc.* **1999**, *121*, 10239−10240. (h) Marquis-Rigault, A.; Dupont-Gervais, A.; Baxter, P. N. W.; Van Dorsselaer, A.; Lehn, J.-M. *Inorg. Chem.* **1996**, *35*, 2307−2310. (i) Navarro, J. A. R.; Janik, M. B. L.; Freisinger, E.; Lippert, B. *Inorg. Chem.* **1999**, *38*, 426−432. (j) Yamanoi, Y.; Sakamoto, Y.; Kusukawa, T.; Fujita, M.; Sakamoto, S.; Yamaguchi, K. *J. Am. Chem. Soc.* **2001**, *123*, 980−981.

(4) Farrell, J. R.; Mirkin, C. A.; Guzei, I. A.; Liable-Sands, L. M.; Rheingold, A. L. *Angew. Chem., Int. Ed.* **1998**, *37*, 465−467.

(5) Farrell, J. R.; Mirkin, C. A.; Liable-Sands, L. M.; Rheingold, A. L. *J. Am. Chem. Soc.* **1998**, *120*, 11834−11835.

(6) Holliday, B. J.; Farrell, J. R.; Mirkin, C. A.; Lam, K.-C.; Rheingold, A. L. *J. Am. Chem. Soc.* **1999**, *121*, 6316−6317.

(7) (a) Farrell, J. R.; Eisenberg, A. H.; Mirkin, C. A.; Guzei, I. A.; Liable-Sands, L. M.; Incarvito, C. D.; Rheingold, A. L.; Stern, C. L. *Organometallics* **1999**, *18*, 4856−4868. (b) Indeed, the direct reaction of the Rh(I) transition metal starting material with ligand (**7**) in the presence of a coordinating small molecule (i.e. CH_3CN) results in the formation of insoluble oligomers. When this same reaction mixture is heated to 80 °C for 3.5 days we see quantitative formation of monomer **12** as confirmed by $^{31}P\{^1H\}$ NMR spectroscopy (see Supporting Information). This demonstrates the necessity of the weak-links to direct the formation of discrete closed rings in high yield via chelation.

(8) Dixon, F. M.; Eisenberg, A. H.; Farrell, J. R.; Mirkin, C. A.; Liable-Sands, L. M.; Rheingold, A. L. *Inorg. Chem.* **2000**, *39*, 3432−3433.

(9) Eisenberg, A. H.; Dixon, F. M.; Mirkin, C. A.; Stern, C. L.; Incarvito, C. D.; Rheingold, A. L. *Organometallics* **2001**, *20*, 2052−2058.

(10) (a) Liu, X.; Eisenberg, A. H.; Stern, C. L.; Mirkin, C. A. *Inorg. Chem.* **2001**, *40*, 2940−2941. (b) Liu, X.; Stern, C. L.; Mirkin, C. A. *Organometallics* **2002**, *21*, 1017−1019. (c) Ovchinnikov, M. V.; Holliday, B. J.; Mirkin, C. A.; Zakharov, L. N.; Rheingold, A. L. *Proc. Natl. Acad. Sci. U.S.A.* **2002**, *99*, 4927−4931.

(11) (a) Slone, C. S.; Weinberger, D. A.; Mirkin, C. A. In *Progress In Inorganic Chemistry*; Karlin, K. D., Ed.; John Wiley & Sons: New York, 1999; Vol. 48, pp 233−350. (b) Bader, A.; Lindner, E. *Coord. Chem. Rev.* **1991**, *108*, 27−110.

Scheme 2

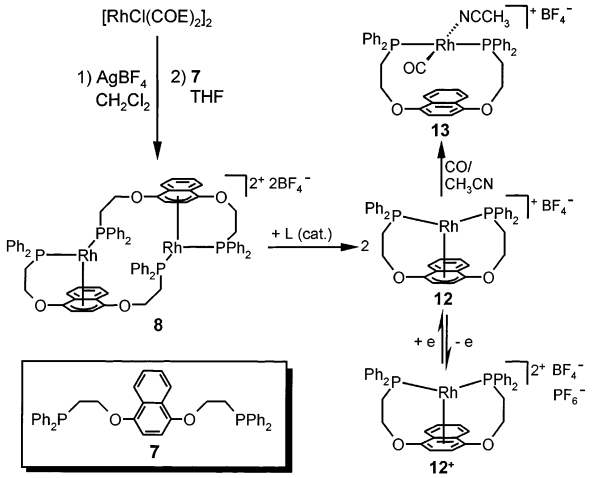

Scheme 3

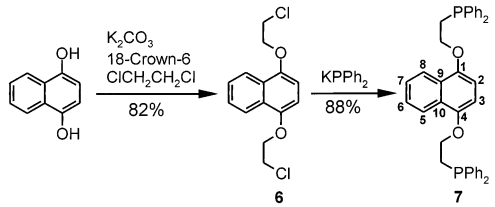

facile conversion to the thermodynamic mononuclear product. Therefore, one can study the kinetics of conversion of condensed intermediates formed from **7** into the respective mononuclear thermodynamic product to gain insight into some of the important mechanistic factors underlying this process.

Results

The new unsymmetric ligand **7**, 1,4-bis(2-diphenylphosphinoethoxy)naphthalene, was synthesized in two steps. First, 1,4-dihydroxynaphthalene was reacted with excess 1,2-dichloroethane in the presence of anhydrous potassium carbonate and a catalytic amount of 18-crown-6 in refluxing acetone to give 1,4-di(2-chloroethoxy)naphthalene **6**. Second, the alkoxy-chloro derivative **6** was converted to the corresponding diphenylphosphine **7** by reacting it with $KPPh_2$ in THF (Scheme 3). All spectroscopic, high-resolution mass spectrometry and combustion analysis data for **6** and **7** are consistent with the proposed structures (vide infra).

The binuclear Rh(I) slipped intermediate **8** was synthesized in near-quantitative yield by reacting ligand **7** in THF with a Rh(I) precursor generated by the reaction of $[RhCl(COE)_2]_2$ and $AgBF_4$ in dichloromethane at room temperature (Scheme 2). This method is analogous to those used for preparing compounds **2a** and **3b** from Rh(I) and their respective ligands (Scheme 1).[4−8] Notably, this reaction yields the slipped isomeric product **8** with no observation of the bow-tie product containing arene rings stacked directly on top of one another (Scheme 1).

Solution Characterization of 8. The ^1H NMR spectrum of the condensed intermediate **8** reflects the unsymmetric nature of the proposed solution and determined solid-state structures (vide infra). The protons of the methylene arms between the phosphorus and ethoxyaryl chelates yield eight distinct resonances in the 1-D proton spectrum. Additionally, the aromatic region displays multiple resonances associated with the break in symmetry of the naphthalene ring in this coordination environment. The COSY spectrum of **8** in CD_2Cl_2 was taken to elucidate the complicated shifts and couplings shown in the standard proton experiment (see Supporting Information). On the basis of the correlation peaks in the COSY spectrum, the methylene resonances of the carbons adjacent to the phosphorus (1.7−2.7 ppm) and oxygen (3.7−5.4 ppm) atoms have been unambiguously assigned (see Experimental Section). All of the methylene resonances display coordination shifts (Δ_{coord}) between ±0.1 and 1.3 ppm.

To confirm the methylene assignments and aid in the analysis of the aromatic region of the ^1H NMR spectrum, the $^{13}C\{^1H\}$ NMR and HMQC (see Supporting Information) spectra were recorded. The $^{13}C\{^1H\}$ NMR spectrum of **8** displays distinct resonances for each carbon in the ligand skeleton. The carbons adjacent to the phosphorus atom display the expected C−P coupling with coupling constants on the order of 30 Hz. Interestingly, of the other carbons within three bonds of the phosphorus atom, only the carbons on the chelated portion of the ligand display further C−P coupling ($^2J_{P-C-C}$ and $^2J_{P-Rh-C}$), consistent with a Karplus-type effect.[12,13] The $^{13}C\{^1H\}$ NMR spectrum of **8** shows large Δ_{coord} values for the carbon resonances of the 1/4 and 2/3 position carbon atoms of the naphthalene ring relative to free ligand, 30 and 20 ppm, respectively. The 9/10 carbon resonances show only a minimal shift of 3 ppm. The large shifts in the observed resonances of carbons 1−4 are consistent with a preference for an η^4-bonding interaction for the naphthalene rings,[14] as observed in the solid-state structure (vide infra).

$^{31}P\{^1H\}$ NMR spectroscopy of **8** shows two resonances at 25.7 (dd, J_{P-P} = 40 Hz, J_{Rh-P} = 205 Hz) and 34.9 ppm (dd, J_{P-P} = 40 Hz, J_{Rh-P} = 216 Hz) in dichloromethane-d_2. These chemical shifts, splitting patterns, and coupling constants are characteristic of slipped intermediate structures, which consist of Rh(I) metal centers with two-legged piano-stool geometries.[7] Even though the arene−Rh(I) interaction in bisphosphine Rh(I) complexes with two-legged piano-stool geometries is known to be relatively weak,[15] ring slippage or other fluxional behavior associated with the naphthalene rings of **8**, if they occur, are too fast to be observed on the $^{31}P\{^1H\}$ NMR time scale in the temperature range between −60 and +70 °C.

(12) (a) Samitov, Y.; Safiullin, R. K. *Zh. Obshch. Khim.* **1988**, *58*, 983−989. (b) Lazhko, É. I.; Luzikova, E. V.; Mikhailov, G. Y.; Kazankova, M. A.; Ustynyuk, Y. A. *Zh. Obshch. Khim.* **1988**, *58*, 1247−1258. (c) Ernst, L. *Org. Magn. Reson.* **1977**, *9*, 35−43. (d) Kainosho, M. *J. Phys. Chem.* **1970**, *74*, 2853−2855.

(13) (a) Lambert, J. B.; Shurvell, H. F.; Verbit, L.; Cooks, R. G.; Stout, G. H. *Organic Structural Analysis*; Macmillan Publishing: New York, 1976. (b) Karplus, M. *J. Chem. Phys.* **1959**, *30*, 11−15. (c) Karplus, M. *J. Am. Chem. Soc.* **1963**, *85*, 2870−2871. (d) Gutowsky, H. S.; Karplus, M.; Grant, D. M. *J. Chem. Phys.* **1959**, *31*, 1278−1289.

(14) (a) Müller, J.; Gaede, P. E.; Hirsch, C.; Qiao, K. *J. Organomet. Chem.* **1994**, *472*, 329−335. (b) Schäufele, H.; Hu, D.; Pritzkow, H.; Zenneck, U. *Organometallics* **1989**, *8*, 396−401. (c) Bennett, M. A.; Lu, Z.; Wang, X.; Bown, M.; Hockless, D. C. R. *J. Am. Chem. Soc.* **1998**, *120*, 10409−10415. (d) Crabtree, R. H.; Parnell, C. P. *Organometallics* **1984**, *3*, 1727−1731. (e) Rieke, R. D.; Henry, W. P.; Arney, J. S. *Inorg. Chem.* **1987**, *26*, 420−427. (f) Chin, R. M.; Dong, L.; Duckett, S. B.; Jones, W. D. *Organometallics* **1992**, *11*, 871−876.

(15) Singewald, E. T.; Shi, X.; Mirkin, C. A.; Schofer, S. J.; Stern, C. L. *Organometallics* **1996**, *15*, 3062−3069.

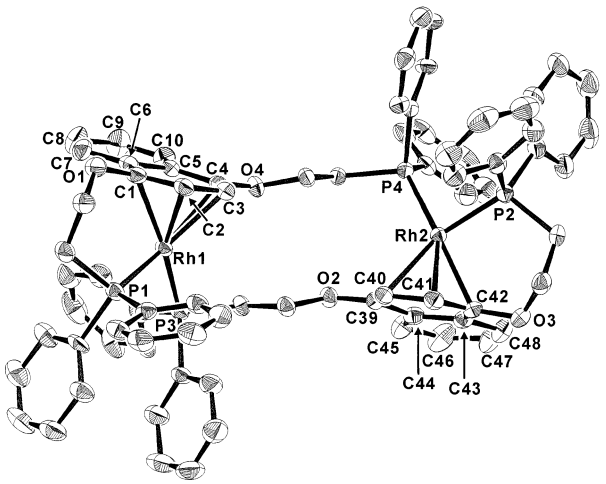

Figure 1. ORTEP diagram of complex **8**. Thermal ellipsoids are drawn at the 50% probability level. Hydrogen atoms, solvent molecules, and anions are omitted for clarity. See Table 1 for selected bond distances and angles.

X-ray Crystallography of 8. The slipped arene configuration of **8** was confirmed by X-ray crystallography (Figure 1). Pale red single crystals suitable for X-ray analysis were grown by slow diffusion of ether into a dichloromethane solution of **8**. One dichloromethane and a diethyl ether molecule were cocrystallized with **8** but exhibited severe disorder. Therefore, they were refined isotropically, while the remaining nonhydrogen atoms were refined anisotropically. The selected bond lengths and angles are given in Table 1. In the solid state, the two naphthalene rings of **8** exhibit a syn conformation, and the observed Rh−C distances are in the range for Rh(I) compounds with bis(phosphine), η^6-arene piano-stool geometries (Rh−C = 2.217−2.516 Å).[16,17] However, the naphthalene ring interaction with the Rh(I) metal center might best be described as η^4 rather than η^6 since there are three short, one medium, and two long interatomic Rh−C distances: Rh(1)−C(1) = 2.261(6) Å, Rh(1)−C(2) = 2.211(6) Å, Rh(1)−C(3) = 2.298(6) Å, Rh(1)−C(4) = 2.419(6) Å, Rh(1)−C(5) = 2.569(6) Å, Rh(1)−C(6) = 2.507(6) Å, Rh(2)−C(39) = 2.482(6) Å, Rh(2)−C(40) = 2.360(6) Å, Rh(2)−C(41) = 2.253(6) Å, Rh(2)−C(42) = 2.265(6) Å, Rh(2)−C(43) = 2.514(6) Å, Rh(2)−C(44) = 2.622(6) Å. While the η^4 hapticity in structures **8** and **12** (vide infra) is less pronounced than in other naphthalene-containing systems as judged by the relatively small hinge angles (6° and 8°, respectively) and 10% difference in bound and unbound Rh−C bond lengths,[14] the Rh(I) metal center displays an off-center distortion in its coordination to the naphthalene ring that is statistically meaningful and also displayed in the solution NMR studies. The two rhodium metal centers are separated by 7.45 Å. The Rh−P bond lengths (Rh−P(chelating)$_{ave}$ = 2.236 Å and Rh−P(bridging)$_{ave}$ = 2.267 Å) are slightly shorter than that of the benzene analogue, [μ^2,η^1:η^6:η^1-(1,4-(Ph$_2$PCH$_2$CH$_2$O)$_2$C$_6$H$_4$)$_2$Rh$_2$][BF$_4$]$_2$ (Rh−P(chelating)$_{ave}$ = 2.274 Å) and (Rh−P(bridging)$_{ave}$ = 2.296 Å); therefore, the average P−Rh−P bond angle (95.38°) is slightly larger than that of the analogue (95.06°).[7]

Reactivity of 8. Upon addition of acetonitrile to a dichloromethane-d_2 solution of **8**, the weak Rh−arene linkages are selectively cleaved to form a series of open macrocycles (**9a**−**d**), which are structural and coordination isomers of each other (Scheme 4). ^{31}P{^{1}H} NMR spectroscopy of mixture **9** shows four doublets: two at 39.1 (d, J_{Rh-P} = 173 Hz) and 37.3 ppm (d, J_{Rh-P} = 173 Hz) for the *cis*-acetonitrile complexes **9a**,**b**, and two at 24.4 (d, J_{Rh-P} = 131 Hz) and 24.1 ppm (d, J_{Rh-P} = 131 Hz) for the *trans*-CH$_3$CN-Rh(I)-NCCH$_3$ complexes **9c**,**d** in a 13:4:2:1 ratio, respectively. These resonances are assigned as the four structures that can result from the combination of syn- and anti-conformations of the naphthalene rings and the cis- and trans-coordination modes of the phosphine and acetonitrile ligands (Scheme 4). The syn- and anti-confirmations of each pair of coordination isomers could not be unambiguously differentiated in solution. The formation of cis- and trans-isomers with this class of compounds has been observed with analogous macrocycles, and the spectroscopy for those compounds compares well with that for the cis- and trans-compounds in mixture **9**.[15,18−20] Interestingly, mixture **9** consists of the coordination and conformational isomers associated with the different orientations of the arene rings and the ligand environment around the metal center. In contrast, the two macrocycles with strictly *trans*-phosphine coordination, **10** and **11** (vide infra), exist as single well-characterized products. This can be explained by considering the arene−arene distance in each system. In X-ray diffraction studies of a bis-acetonitrile (cis-) adduct analogous to **9**[9] and **9** (*cis*-, *anti*-) (vide infra), the average arene−arene distance is 4.05 Å in comparison to an average of 6.37 Å for **11** and three other macrocycles previously reported.[7−9] The increased arene−arene distance allows for free rotation about the 1,4-axis of the naphthalene rings in complexes **10** and **11** and therefore scrambling of the isomers on the NMR time scale. When the solvent was evaporated in vacuo and the resulting residue redissolved in dichloromethane-d_2, slipped intermediate **8** can be recovered cleanly as evidenced by ^{31}P{^{1}H} NMR spectroscopy.

When a dichloromethane-d_2 solution of slipped intermediate **8** is charged with CO (1 atm) the color changes from deep red to pale yellow with the concomitant formation of a white precipitate (Scheme 4). The ^{31}P{^{1}H} NMR spectrum of the supernatant shows only one broad doublet at 26.8 ppm with J_{Rh-P} = 90 Hz. This compares well with the ^{31}P{^{1}H} NMR resonances for the analogous trigonal-bipyramidal Rh(I) complexes which have three equatorial CO ligands and two apical phosphine ligands: [(η^1-PhO(CH$_2$)$_2$PPh$_2$)$_2$(CO)$_3$ Rh][BF$_4$], 31.5 ppm (d, J_{Rh-P} = 71.7 Hz); [(μ^2-(1,4-(Ph$_2$PCH$_2$CH$_2$O)$_2$-2,3,5,6-((CH$_3$)$_4$C$_6$)))$_2$(CO)$_6$ Rh$_2$][BF$_4$]$_2$, 20 ppm (d,

(16) (a) Slone, C. S.; Mirkin, C. A.; Yap, G. P. A.; Guzei, I. A.; Rheingold, A. L. *J. Am. Chem. Soc.* **1997**, *119*, 10743−10753. (b) Alvarez, M.; Lugan, N.; Donnadieu, B.; Mathieu, R. *Organometallics* **1995**, *14*, 365−370. (c) Westcott, S. A.; Taylor, N. J.; Marder, T. B.; Baker, R. T.; Jones, N. J.; Calabrese, J. C. *Chem. Commun.* **1991**, 304−305. (d) Townsend, J. M.; Blount, J. F. *Inorg. Chem.* **1981**, *20*, 269−271. (e) Albano, P.; Aresta, M.; Manassero, M. *Inorg. Chem.* **1980**, *19*, 1069−1072.

(17) Singewald, E. T.; Slone, C. S.; Stern, C. L.; Mirkin, C. A.; Yap, G. P. A.; Liable-Sands, L. M.; Rheingold, A. L. *J. Am. Chem. Soc.* **1997**, *119*, 3048−3056.

(18) Singewald, E. T.; Mirkin, C. A.; Levy, A. D.; Stern, C. L. *Angew. Chem., Int. Ed. Engl.* **1994**, *33*, 2473−2475.

(19) Sassano, C. A.; Mirkin, C. A. *J. Am. Chem. Soc.* **1995**, *117*, 11379−11380.

(20) Appleton, T. G.; Clark, H. C.; Manzer, L. E. *Coord. Chem. Rev.* **1973**, *10*, 335−422.

Table 1. Selected Bond Distances (Å) and Bond Angles (deg) for 8, 9 (*cis*-, *anti*-), 11, and 12

8		9 (*cis*-, *anti*-)		11		12	
Rh1−P1	2.2286(15)	Rh1−P1	2.450(15)	Rh1−P1	2.3468(9)	Rh1−P1	2.262(7)
Rh1−P3	2.2675(16)	Rh1−P2	2.2412(15)	Rh1−P2	2.3281(8)	Rh1−P2	2.248(7)
Rh2−P2	2.2438(16)	Rh1−N1	2.050(5)	Rh1−C39	1.824(4)	Rh1−C1	2.261(3)
Rh2−P4	2.2669(15)	Rh1−N2	2.039(5)	Rh1−N1	2.044(3)	Rh1−C2	2.265(2)
Rh1−C1	2.261(6)	N1−C39	1.137(9)	C39−O3	1.141(4)	Rh1−C3	2.253(2)
Rh1−C2	2.211(6)	N2−C41	1.146(10)	C40−N1	1.130(5)	Rh1−C4	2.252(2)
Rh1−C3	2.298(6)	C39−C40	1.460(11)	C40−C41	1.466(6)	Rh1−C5	2.486(3)
Rh1−C4	2.419(6)	C41−C42	1.465(11)	P1−Rh1−P2	174.31(4)	Rh1−C10	2.473(3)
Rh1−C5	2.569(6)	P1−C21	1.842(6)	P1−Rh1−N1	89.95(8)	O1−C1	1.355(4)
Rh1−C6	2.507(6)	P1−C15	1.836(6)	P1−Rh1−C39	92.24(11)	O2−C4	1.373(3)
Rh2−C39	2.482(6)	P2−C27	1.831(6)	P2−Rh1−N1	90.43(8)	C1−C2	1.406(4)
Rh2−C40	2.360(6)	P2−C33	1.825(6)	P2−Rh1−C39	87.45(11)	C2−C3	1.399(4)
Rh2−C41	2.253(6)	P1−Rh1−P2	96.21(5)	C39−Rh1−N1	177.71(13)	C3−C4	1.401(4)
Rh2−C42	2.265(6)	P1−Rh1−N1	175.69(18)	Rh1−C39−O3	177.1(3)	C4−C5	1.444(3)
Rh2−C43	2.514(6)	N2−Rh1−N1	85.9(2)	Rh1−N1−C40	176.3(3)	C5−C10	1.426(3)
Rh2−C44	2.622(6)	N2−Rh1−P2	169.44(14)	N1−C40−C41	178.8(5)	C1−C10	1.460(4)
P1−Rh1−P3	95.82(6)	N1−Rh1−P2	86.76(16)			P1−Rh1−P2	98.05(2)
P2−Rh2−P4	94.94(6)	N2−Rh1−P1	91.52(14)				

Scheme 4

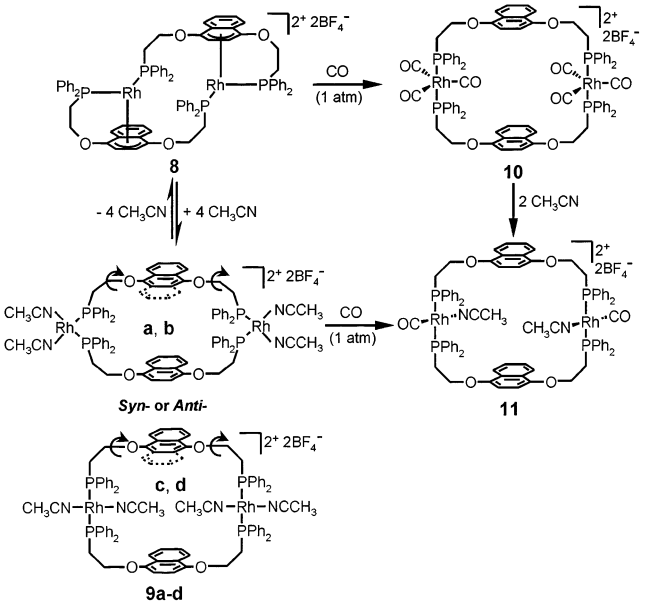

$J_{Rh-P} = 88$ Hz); $[(\mu^2\text{-}(1,4\text{-}(Ph_2PCH_2CH_2O)_2C_6H_4))_2(CO)_6Rh_2][BF_4]_2$, 28.0 ppm (d, $J_{Rh-P} = 78$ Hz); $[(\mu^2\text{-}(4,4'\text{-}(Ph_2PCH_2CH_2O)_2\text{-}C_6H_4\text{-}C_6H_4))_2(CO)_6Rh_2][BF_4]_2$, 30.2 ppm (d, $J_{Rh-P} = 79$ Hz).[7,15] The CO complex was not stable under ESI (electrospray ionization) mass spectrometry conditions, thus precluding the gas-phase characterization of the parent ion. However, a fragment of the macrocycle with the loss of the 6 CO ligands, $[M - 6CO - BF_4^-]^+ = m/z$ 1461.6, was observed. The FTIR spectrum of **10** in dichloromethane-d_2 exhibits two ν_{CO} bands at 2013 (s) and 2093 (s) cm^{-1}, consistent with the proposed structure. The white precipitate (mentioned above) is compound **10** and can be redissolved in dichloromethane saturated with CO.

Complex **10** was collected by filtration over Celite and redissolved in acetonitrile (Scheme 4). As acetonitrile was added, evolution of CO gas was observed. $^{31}P\{^1H\}$ NMR spectroscopy shows the disappearance of the doublet assigned to **10** and the formation of a new doublet at 27.5 ppm ($J_{Rh-P} = 118$ Hz), which has been assigned to the acetonitrile/CO adduct complex **11**. The $^{31}P\{^1H\}$ NMR chemical shift and Rh−P coupling constant correspond well with the analogous data for related *trans*-CO-Rh(I)-$NCCH_3$ complexes.[4,7,15,21] Complex **11** was also synthesized in quantitative yield by addition of CO gas (1 atm) to a dichloromethane-d_2 solution of **9** (Scheme 4).

The ^1H NMR spectra of compounds **9** and **10** are broad, indicating the presence of additional isomers, bonding conformations, or fluctuations that are not resolved on the NMR time scale. However, due to the conformational stability of complex **11**, the ^1H NMR spectroscopy signals are sharp and well-resolved, which allows more detailed analysis of the resonances and their corresponding shifts relative to free ligand **7**. The ^1H NMR spectroscopy resonance associated with the methylene protons in the position α to the phosphine in **11** was shifted downfield by 0.5 ppm relative to **7** via an inductive effect of Rh(I)−P coordination, and the proton signals of the naphthalene ring were shifted upfield presumably due to the shielding effect of the naphthalene rings on each other.

The two naphthalene rings in complexes **9**, **10**, and **11** can have three different conformations analogous to related organic cyclophanes: syn-, anti-, or edge-face.[22] The ^1H NMR spectrum of **11** displays three resonances for the protons on the naphthalene ring. These signals are all shifted upfield relative to the free ligand, indicating that there is significant overlap between the two aromatic rings in solution. More specifically, a comparison between the signals of free ligand **7** and macrocycle **11** yields a cyclization shift (Δ_{cyc}) for each set of protons. The Δ_{cyc} for the protons on C2 and C3 is 0.14, that for C5 and C8 is 0.24, and that for C6 and C7 is 0.22 (see numbering in Scheme 3). The perturbation of all three resonances and the Δ_{cyc} values are consistent with analogous organic *syn*-naphthalenophanes (Δ_{cyc} =

(21) Siedle, A. R.; Gleason, W. B.; Newmark, R. A.; Skarjune, R. P.; Lyon, P. A.; Markell, C. G.; Hodgson, K. O.; Roe, A. L. *Inorg. Chem.* **1990**, *29*, 1667−1673.

(22) (a) Adams, S. P.; Whitlock, H. W. *J. Org. Chem.* **1981**, *46*, 3474−3478. (b) Jarvi, E. T.; Whitlock, H. W. *J. Am. Chem. Soc.* **1980**, *102*, 657−662. (c) Blank, N. E.; Haenel, M. W. *Tetrahedron Lett.* **1978**, 1425−1428. (d) Chandross, E. A.; Ferguson, J.; McRae, E. G. *J. Chem. Phys.* **1966**, *45*, 3546−3553. (e) Katul, J. A.; Zahlan, A. B. *J. Chem. Phys.* **1967**, *47*, 1012−1014. (f) Haigh, C. W.; Mallion, R. B. *Org. Magn. Reson.* **1972**, *4*, 203−228. (g) Chandra, A. K. *Chem. Phys. Lett.* **1970**, *5*, 229−231. (h) Murakami, Y.; Aoyama, Y.; Kida, M.; Nakano, A.; Dobashi, K.; Tran, C. D.; Matsuda, Y. *J. Chem. Soc., Perkin Trans. 1* **1979**, 1560−1567. (i) Shinmyozu, T.; Inazu, T.; Yoshino, T. *Chem. Lett.* **1978**, 405−408. (j) Kawabata, T.; Shinmyozu, T.; Inazu, T.; Yoshino, T. *Chem. Lett.* **1979**, 315−318.

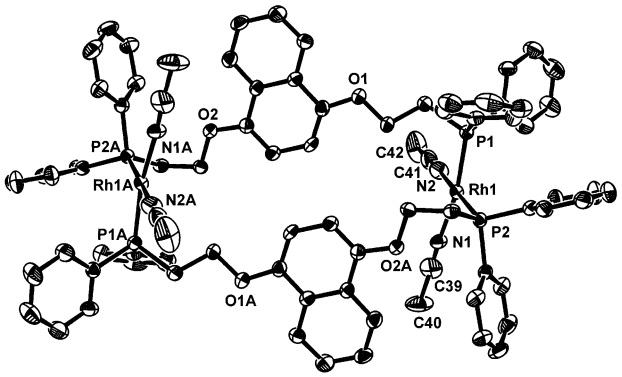

Figure 2. ORTEP diagram of complex **9** (*cis*-, *anti*-). Thermal ellipsoids are drawn at the 50% probability level. Hydrogen atoms, solvent molecules, and anions are omitted for clarity. See Table 1 for selected bond distances and angles.

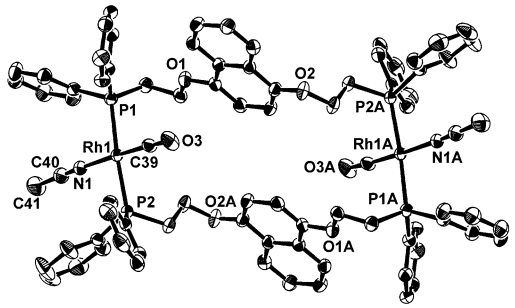

Figure 3. ORTEP diagram of complex **11**. Thermal ellipsoids are drawn at the 50% probability level. Hydrogen atoms, solvent molecules, and anions are omitted for clarity. See Table 1 for selected bond distances and angles.

0−0.2 ppm), indicating that macrocycle **11** displays a syn-conformation of the naphthalene rings relative to one another.[22] Interestingly, even though the spectroscopic data suggest that the naphthalene rings of **11** are in the syn-conformation in solution, the solid-state structures of **9** (*cis*-, *anti*-) and **11** display an anti, displaced, and nearly parallel planar conformation of the naphthalene rings (Figures 2 and 3). This conformational change is presumably due to crystal packing effects maximizing intermolecular $\pi-\pi$ interactions.

X-ray Crystallography of 9 (*cis*-, *anti*-). Slow diffusion of pentane into a concentrated 5:1 dichloromethane:acetonitrile solution containing complexes **9a**−**d** yielded pale yellow crystals suitable for X-ray diffraction analysis. Interestingly, only one of the four conformers/isomers present in the solution mixture **9** is observed in the solid-state structure (Figure 2). The *cis*-phosphine, *cis*-acetonitrile complex of the *anti*-naphthalene conformation **9** (*cis*-, *anti*-) cocrystalized with two molecules of methylene chloride and two molecules of water. The solvent molecules were severely disordered and therefore treated in the data analysis by the SQUEEZE correction method. The remaining non-hydrogen atoms were refined anisotropically, and selected bond distances and angles can be found in Table 1. The naphthalene rings are situated anti to one another in a parallel-planar orientation but do not overlap, demonstrating a lack of intramolecular $\pi-\pi$ interactions in the solid state. The two rhodium(I) metal centers are 11.19 Å apart and display slightly distorted square-planar coordination geometries (L1−Rh−L2 angles of 85.9−96.2°, Table 1). The planes defined by each metal center and its ligands are parallel planar with the acetonitrile ligands pointing to opposite sides of the macrocyclic ring (Figure 2).

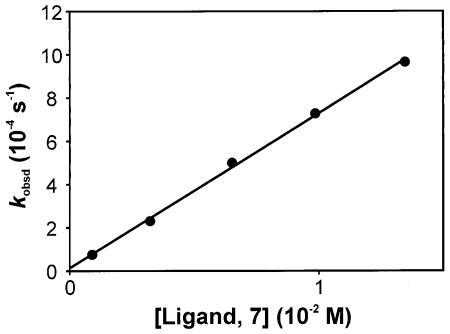

Figure 4. Plot of k_{obsd} vs concentration of **7** for the conversion of **8** to **12** at $T = 40$ °C.

X-ray Crystallography of 11. Yellow single crystals suitable for X-ray diffraction analysis were obtained by layering diethyl ether over an acetonitrile solution of **11** (Figure 3 and Table 1). The X-ray diffraction data show that complex **11** is located on a crystallographic 2-fold axis. Although two acetonitrile molecules cocrystallized with **11**, there is no evidence of any interaction between these solvent molecules and the Rh(I) metal centers. The two naphthalene rings are anti to one another and parallel planar but do not overlap (displaced by over 3 Å), and therefore do not exhibit evidence of intramolecular $\pi-\pi$ interactions in the solid state. The coordination spheres of the rhodium metal centers are best described as distorted square planar with *trans*-bisphosphines (P(1)−Rh(1)−P(2) = 174.31-(4)°) and *trans*-CO, CH_3CN (C(39)−Rh(1)−N(1) = 177.71-(13)°) as predicted by $^{31}P\{^1H\}$ NMR spectroscopy in solution. The two rhodium metal centers are separated by 11.56 Å comparable to that of a related duranyl complex ($[(\mu^2$-(1,4-$(Ph_2PCH_2CH_2O)_2$-2,3,5,6-$((CH_3)_4C_6)))_2$-$(CO)_2(CH_3CN)_2Rh_2][BF_4]_2$, 11.61 Å).[7]

Conversion of Binuclear Complex 8 to Mononuclear Complex 12. The conversion of the slipped intermediate **8** into the analogous mononuclear pianostool complex **12** was studied to gain insight into the relative stabilities of Rh(I) complexes and mechanistic information about this process (Scheme 2). The analogous conversion process has been observed for related ligand systems but never studied in detail.[2,7] The conversion of **8** to **12** was monitored by ^1H and $^{31}P\{^1H\}$ NMR spectroscopy with no sign of decomposition or side reactions. Kinetic studies based on ^1H NMR spectroscopy were undertaken in the presence of phosphorus-based ligands. The latter catalyze the associative dinuclear to mononuclear conversion process. The kinetics reveal first-order dependence on macrocycle (**8**) concentration, and the plot of k_{obsd} vs [**7**] shows a linear relationship with a zero intercept (Figure 4). The rate of the conversion was studied over a 30−50 °C temperature range in the presence of ligand **7** (Figure 5A). From these data, the activation parameters have been determined for the conversion (Figure 5A, inset). Additionally, the kinetics of the conversion of **8** into **12** were performed in the presence of a series of phosphines of varying steric and electronic parameters (Table 2).

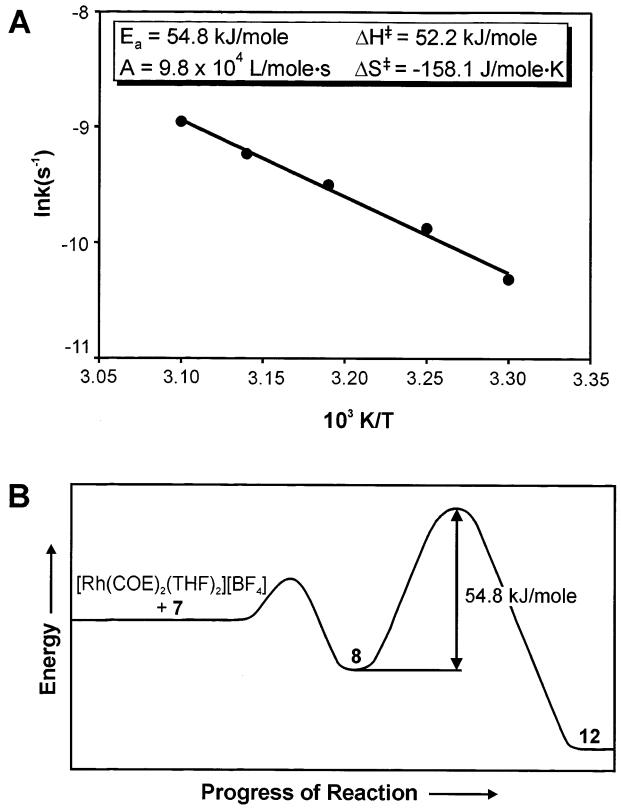

Figure 5. (A) Temperature profile of the rate constants for the conversion of **8** to **12** in the presence of excess ligand **7** plotted according to the Arrhenius model. The inset shows the calculated activation parameters for this reaction. (B) The reaction coordinate diagram profiling the formation and catalyzed conversion of binuclear intermediate structure **8** to the mononuclear thermodynamic product, **12**.

Table 2. Effect of Phosphine Ligand on k_{obsd} of 8 to 12 Conversion[a]

entry	ligand	k_{obsd} (10^{-5} s^{-1})	cone angle (deg)
a	PBu_3	7.52	132
b	PCy_3	1.08	170
c	$PEtPh_2$	4.42	140
d	PPh_3	3.98	145
e	$P(C_6F_5)_3$	0.558	184
f	$P(OMe)Ph_2$	6.97	132
g	BDPO[b]	5.93	140[c]
h	**7**	7.47	

[a] The conversion of **8** to **12** was measured in CD_2Cl_2 at $T = 40$ °C in the presence of 0.2 equiv of monophosphine (a−f) or 0.1 equiv of diphosphine (g and h) by ^1H NMR spectroscopy against a decane internal standard. [b] Bis(1,8-diphenylphosphino)octane. [c] Estimated based on $PEtPh_2$.

Solution Characterization of 12. To elucidate the solution structure of **12** and make a complete assignment of the one-dimensional ^1H and $^{13}C\{^1H\}$ NMR spectra, the H,H-COSY and two-dimensional H,C-HMQC (see Supporting Information) spectra were recorded in CD_2Cl_2. The splitting of each methylene peak into two distinct resonances in the ^1H NMR spectrum of **12** is diagnostic of the lack of symmetry about the O−Rh−O plane. All of the methylene resonances (a/a′ and b/b′) are broad with unresolved coupling; however, the COSY spectrum of **12** displays the expected correlations of a to a′ and b to b′ for methylene protons on the same carbon atom (Figure 6). The

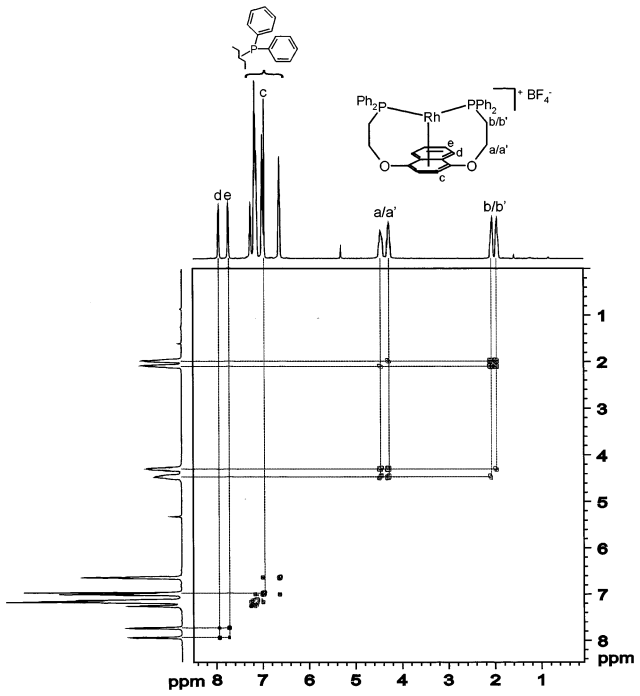

Figure 6. COSY spectrum (500 MHz) of monomer **12** in CD_2Cl_2 shown as a contour plot. The 500-MHz one-dimensional ^1H NMR spectrum is shown at the top and left-hand edge. The signals that can be assigned are marked accordingly. The dashed lines highlight peak correlations.

adjacent aromatic protons, d and e (7.6−8.0 ppm), display the expected correlations as well. The remaining nondiphenylphosphine proton, c, displays a singlet resonance at 6.96 ppm with a self-correlated peak in the COSY spectrum. The resonances associated with protons a/a′ and c display significant coordination shifts (Δ_{coord}) of −0.7 and +0.4 ppm Δ_{coord} (respectively), which are consistent with the proposed solution and solid-state structures.

The rigid nature of **12** is confirmed by the observation of only single correlations between the methylene protons on adjacent carbons (a to b only), a demonstration of the Karplus effect in this system.[13] For example, based on the X-ray structure of **12** (vide infra), the dihedral angles between the proton labeled a and the protons on the adjacent carbon, b and b′, are 169° and −76° (respectively). According to the Karplus relationship, the coupling of the vicinal ($^3J_{H-C-C-H}$) spins a to b should be ∼9.5 Hz, and a to b′ should not exhibit spin−spin coupling. This correlation pattern is observed in the COSY spectrum of **12** indicating a high level of agreement between the solution and solid-state structures. Identical analyses can be performed for the remaining seven methylene protons, and all dihedral angle/spin−spin coupling relationships agree with the observed data.

By comparing the $^{13}C\{^1H\}$ NMR spectrum of **12** with the $^{13}C\{^1H\}$ NMR spectrum of free ligand and analyzing the ^1H NMR (vide infra) and HMQC spectrum of **12** (see Supporting Information), the complete assignment of the $^{13}C\{^1H\}$ NMR spectrum of **12** has been made. The HMQC spectrum displays the expected correlations between the assigned ^1H NMR spectrum and the $^{13}C\{^1H\}$ NMR resonances. All carbon resonances show a

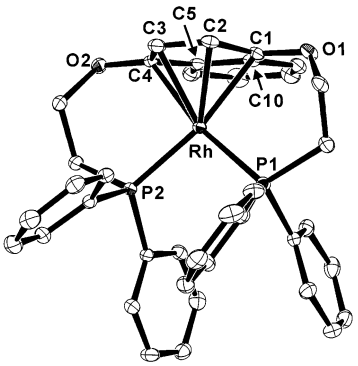

Figure 7. ORTEP diagram of complex **12**. Thermal ellipsoids are drawn at the 50% probability level. Hydrogen atoms, solvent molecules, and anions are omitted for clarity. See Table 1 for selected bond distances and angles.

relatively small Δ_{coord} (±3−6 ppm) except for the two resonances of the carbons directly bound to the metal center, which display a Δ_{coord} of −17 ($C_{1/4}$) and −32 ($C_{2/3}$) ppm. These coordination shifts and assignments are consistent with assignments for previously studied η^4-coordination modes for untethered naphthalene ligands and confirm the η^4-coordination of the arene ring to the Rh(I) in **12** in solution.[14] In addition to the peak positions and shifts, the observed coupling patterns are also consistent with the proposed solution structure. The resonance associated with the carbon atoms adjacent to the phosphorus atoms displays a second-order coupling pattern that can be modeled as a AXY system indicating the expected coupling to the adjacent phosphorus atom as well as the ^{103}Rh metal center, $^2J_{Rh-P-C}$. The resonances assigned to the carbons that are directly interacting with the Rh(I) metal center in an η^4-fashion both display the expected ^{103}Rh−^{13}C spin−spin coupling (J_{Rh-C}) of 3−4 Hz, which is in agreement with previously reported carbon atoms π-bound to Rh(I).[23] The lack of a large Δ_{coord} and Rh−C coupling for carbons 9 and 10 further supports an η^4, as opposed to η^6, coordination mode for the Rh(I) metal center in solution. All of these data are consistent with the proposed structure for complex **12** and demonstrate excellent agreement between the solution and solid-state structures.

X-ray Crystallography of 12. Slow diffusion of pentane into a saturated dichloromethane solution of **12** gave prismatic orange crystals suitable for X-ray diffraction analysis (Figure 7 and Table 1). The observed Rh−C distances are in the expected range for monomeric Rh(I) compounds with a bis(phosphine), η^6-arene piano-stool geometry (Rh−C = 2.217−2.516 Å).[16,17] However, the naphthalene ring is actually bound to the Rh(I) metal center via an η^4-bonding mode rather than η^6-bonding mode as evidenced by two long (Rh(1)−C(5) = 2.486(3) Å, Rh(1)−C(10) = 2.473(3) Å) and four short (Rh(1)−C(1) = 2.261(3) Å, Rh(1)−C(2) = 2.265(2) Å, Rh(1)−C(3) = 2.253(2) Å, Rh(1)−C(4) = 2.252(2) Å) Rh−C bonds. The Rh−P bond lengths (Rh(1)−P_{ave} = 2.2550(7) Å) are slightly longer than that of the duranyl analogue, [(η^1:η^6:η^1-(1,4-($Ph_2PCH_2CH_2O$)$_2$-2,3,5,6-((CH_3)-C_6)))Rh][BF_4] (Rh−P_{ave} = 2.2388(12) Å),[7] presumably due to the trans influence of the naphthalene ring via a strong arene−Rh(I) interaction. This bond distance falls within the range of previously reported mononuclear Rh(I) piano-stool structures (average Rh−P bond lengths = 2.219−2.251 Å).[7,16,17,21] The crystal packing diagram of **12** shows that the naphthalene rings from two independent molecules of **12** do not π−π stack on one another, even though a similar η^6-anthraceno−diphosphine−silver(I) complex displays π−π stacking interactions between the two anthracyl rings in the unit cell (arene−arene distance = 3.416 Å).[24]

Reactivity of Mononuclear Compound 12. The mononuclear Rh(I) piano-stool complex **12** does not show any reactivity with CO or acetonitrile alone in solution (at room temperature) even though the arene−Rh(I) bond is known to be rather weak.[15,18,19] However, when complex **12** was charged with CO in the presence of acetonitrile the color changed from deep red to pale yellow due to the formation of mononuclear *trans*-CO-Rh(I)-$NCCH_3$ complex **13**, which results from the cleavage of this weak arene−Rh(I) interaction (Scheme 2). The $^{31}P\{^1H\}$ NMR spectrum of this solution exhibits a doublet at 23.6 ppm with coupling constant J_{Rh-P} = 117 Hz, which compares well with that for binuclear *trans*-CO-Rh(I)-$NCCH_3$ complex **11** (J_{Rh-P} = 118 Hz) and previously reported related complexes.[4,7,15,21] The ^{1}H NMR spectrum and mass spectroscopy data for **13** are also consistent with the proposed structure. Finally, complex **12** undergoes reversible one-electron oxidation ($E_{1/2}$ = 660 mV vs Fc/Fc^+) forming a stable Rh(II) complex (Scheme 2). This is consistent with what has been observed with other Rh(I) two-legged piano-stool analogues of **12**.[17,18,25]

Discussion

In addition to the reactivity outlined above, ligand **7** and its binuclear Rh(I) complex, **8**, have afforded us the opportunity to study the conversion of binuclear intermediates to mononuclear complexes and to map out some of the possible reaction pathways and energetics associated with the Weak-Link Approach.

As reported previously, for macrocycles prepared via the Weak-Link Approach, the two-legged piano-stool mononuclear Rh(I) complex is often the thermodynamic product with respect to the slipped and bow-tie intermediates (Scheme 1).[7] Since the naphthalene complex, **8**, has the potential to undergo ring-slippage and numerous ligand−metal binding modes available to facilitate ligand substitution, this system is especially well-suited for studying the conversion of dimer **8** to monomer complex **12** (Scheme 2). Notably these transformations are much faster compared to the analogous transformation involving the previously reported durene complex [(η^1:η^6:η^1-(1,4-($Ph_2PCH_2CH_2O$)$_2$-2,3,5,6-((CH_3)-C_6)))Rh][BF_4], which takes 10 d at 75 °C in $ClCD_2CD_2$-Cl to undergo dimer-to-monomer conversion. Additionally, the latter transformation is accompanied by significant decomposition (10−20%).[7]

(23) (a) Bodner, G. M.; Storhoff, B. N.; Doddrell, D.; Todd, L. J. *Chem. Commun.* **1970**, 1530−1531. (b) Arthurs, M.; Gross, P.; Kubal, G.; Paniwnyk, L.; Curzon, E. *J. Organomet. Chem.* **1989**, *366*, 223−243.

(24) Xu, F.-B.; Weng, L.-H.; Sun, L.-J.; Zhang, Z.-Z.; Zhou, Z.-F. *Organometallics* **2000**, *19*, 2658−2660.

(25) Dixon, F. M.; Farrell, J. R.; Doan, P. E.; Williamson, A.; Weinberger, D. A.; Mirkin, C. A.; Stern, C.; Incarvito, C. D.; Liable-Sands, L. M.; Zakharov, L. N.; Rheingold, A. L. *Organometallics* **2002**, *21*, 3091−3093.

Upon extended heating (48 h) of analytically pure **8** under conditions similar to those previously reported (vide supra), no conversion to monomer was observed. However, the addition of a small amount of free ligand **7** to this solution brought about complete conversion within 20 min under identical conditions. In the previously reported system,[7] the small amount of decomposition that was observed provided a small but increasing amount of free phosphine ligand, which we now believe catalyzed the conversion to monomeric product. Given the dependence of the conversion on the presence of excess ligand and the absence of phosphine bound to **12** in the final product mixture, the formation of monomer from binuclear species is thought to be an associative process. With this in mind, we performed kinetic experiments aimed at studying the conversion of dimer **8** to monomer **12** in the presence of 0.1 equiv of free ligand (**7**) between 30 and 50 °C in CD_2Cl_2. The process was monitored by ^1H NMR spectroscopy against a decane internal standard. These experiments all displayed clean first-order kinetics based on macrocycle concentration and a linear temperature dependence,[26] which allowed us to calculate the activation parameters for dimer to monomer conversion (Figure 5). Additionally, the rate of reaction is first order in phosphorus-based nucleophile. The plot of k_{obsd} vs [**7**] is linear with a zero intercept, consistent with an associative process (Figure 4).

The reaction proceeds with a forward activation energy of 54.8 kJ/mol and an activation enthalpy of 52.2 kJ/mol (Figure 5B). This relatively small enthalpy of activation is indicative of a transition state where bond making is closely accompanied by bond breaking, which lends support to the hypothesis that this reaction is associative in nature and that the first steps of ligand binding are rate limiting. The large negative activation entropy (−158.1 J/(mol K)) indicates the formation of a highly ordered transition state, which is consistent with an associative process that brings **8** and 1 equiv of **7** (or 2 equiv of monophosphine) together prior to dissociation to a mononuclear complex. On the basis of these observations and earlier studies of associative substitution reactions at Rh(I) facilitated by ring-slippage of coordinated arene rings,[27−30] we propose a mechanism that involves the sequential and rate determining coordination of incoming ligands to the metal centers of dimer **8**, with concomitant ring slippage of the coordinated arenes from η^4 to η^2 (accommodating the additional ligand and maintaining the 16-electron count on the rhodium metal center) (**14** in Scheme 5). This is followed by dissociation of the bridging phosphine and ring slippage back to an η^4-coordination mode to give 2 equiv of monomeric intermediate, **15**. The observed product **12** can then be formed by associative attack of the free chelating phosphine, again with an η^4 to η^2 change in arene coordination mode, followed by loss of the catalytic phosphine ligand and reestablishment of the η^4-coordination mode (Scheme 5). Consistent with this hypothesis, intermediates cannot be observed even by the addition of excess ethyldiphenylphosphine at −78 °C and gradual warming to room temperature while monitoring by $^{31}P\{^1H\}$ NMR spectroscopy.

Scheme 5

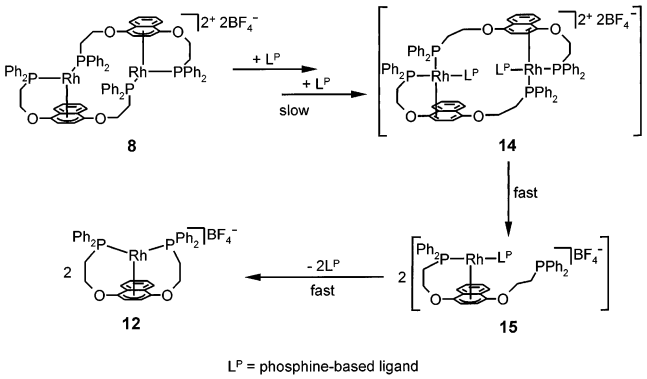

By using different phosphines with systematically varied steric and electronic properties as catalytic reagents, one can gain further insight into this process; specifically, information about the transition state and rate determining step of the reaction can be inferred from effects on the rate of reaction. Six commercially available monodentate phosphines of varying steric and electronic parameters were investigated in addition to the bidentate ligands **7** and bis(1,8-diphenylphosphino)-octane (BDPO) (Table 2).[31] For comparison purposes, 0.2 equiv (consistent equivalent of phosphine) of the monodentate phosphines were added to CD_2Cl_2 solutions of **8**, and the conversion was monitored by ^1H NMR spectroscopy at 40 °C against a decane internal standard. BDPO was used in these experiments in order to test the role of both the chelation effect and the hemilabile nature of ligand **7** to facilitate the conversion of **8** to **12**. BDPO is of comparable P−P length to **7** but lacks the aromatic core and the labile oxygen moieties.

The rate of conversion of condensed intermediate **8** into mononuclear complex **12** varies with the ligand introduced to catalyze the process, but all processes follow first order (in macrocycle) kinetics. The data listed in Table 2 were compared to four parameters for the phosphine ligands, including cone angle,[32,33] electronic parameter (Tolman),[32] QALE sigma donation ability,[34] and basicity.[35] The ligand size, as measured by the cone angle of the phosphines, is the dominate

(26) (a) Espenson, J. H. *Chemical Kinetics and Reaction Mechanisms*, 2nd ed.; McGraw-Hill: New York, 1995. (b) Pilling, M. J.; Seakins, P. W. *Reaction Kinetics*; Oxford University Press: New York, 1995.

(27) (a) Kataoka, Y.; Saito, Y.; Shibahara, A.; Tani, K. *Chem. Lett.* **1997**, 621−622. (b) Calhorda, M. J.; Romão, C. C.; Veiros, L. F. *Chem. Eur. J.* **2002**, *8*, 868−875.

(28) (a) Basolo, F. *New J. Chem.* **1994**, *18*, 19−24. (b) Basolo, F. *Inorg. Chim. Acta* **1985**, *100*, 33−39. (c) Rerek, M. E.; Basolo, F. *J. Am. Chem. Soc.* **1984**, *106*, 5908−5912. (d) Rerek, M. E.; Ji, L.-N.; Basolo, F. *Chem. Commun.* **1983**, 1208−1209.

(29) Rerek, M. E.; Basolo, F. *Organometallics* **1983**, *2*, 372−376.

(30) Zhang, S.; Shen, J. K.; Basolo, F.; Ju, T. D.; Lang, R. F.; Kiss, G.; Hoff, C. D. *Organometallics* **1994**, *13*, 3692−3702.

(31) 1,8-Bis(diphenylphosphino)octane (BDPO) was prepared in 80% yield by the reaction of $KPPh_2$ with 1,8-dibromooctane in THF at room temperature followed by filtration through a plug of alumina and removal of solvent. The crude colorless solid was purified by passing through a short plug of silica gel in CH_2Cl_2 and recrystallizing with pentane at −30 °C. The composition and purity was confirmed by ^1H and $^{31}P\{^1H\}$ NMR spectroscopy as compared to the following: Hill, W. E.; Minahan, D. M. A.; Taylor, J. G.; McAuliffe, C. A. *J. Chem. Soc., Perkin Trans. 2* **1982**, 327−330.

(32) Collman, J. P.; Hegedus, L. S.; Norton, J. R.; Finke, R. G. *Principles and Applications of Organotransition Metal Chemistry*; University Science Books: Mill Valley, CA, 1987.

(33) Tolman, C. A. *Chem. Rev.* **1977**, *77*, 313−348.

(34) (a) Fernandez, A. L.; Wilson, M. R.; Prock, A.; Giering, W. P. *Organometallics* **2001**, *20*, 3429−3435. (b) Fernandez, A. L.; Reyes, C.; Prock, A.; Giering, W. P. *J. Chem. Soc., Perkin Trans. 2* **2000**, 1033−1041.

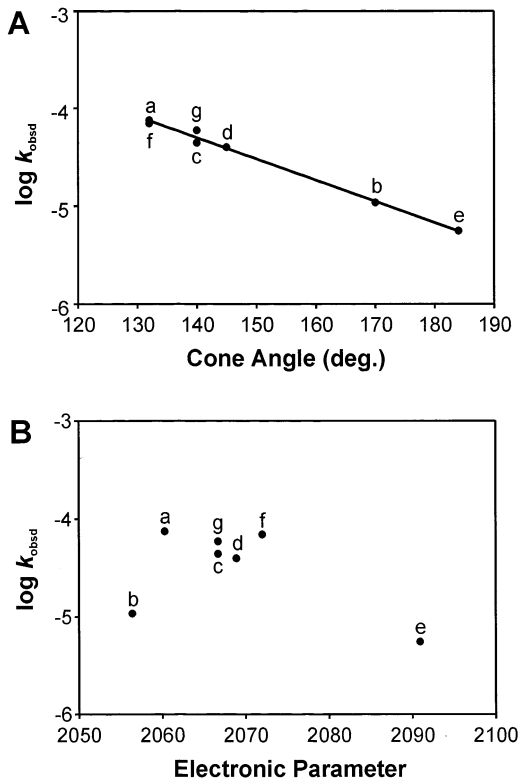

Figure 8. (A) Plot of log k_{obsd} vs cone angle of the phosphorus nucleophile for the conversion of **8** to **12** at T = 40 °C. The letters correspond to those in Table 2. (B) Plot of log k_{obsd} vs the electronic parameter[33] of the phosphorus nucleophile for the conversion of **8** to **12** at T = 40 °C. The letters correspond to those in Table 2.

factor controlling the rate of the reaction, which has been previously observed with associative substitution reactions.[29] A plot of rate of conversion versus cone angle is shown in Figure 8A and indicates a linear correlation between reaction rate and steric bulk of the nucleophile. Other ligand parameters showed poor correlation to the reaction rate data (Figure 8B), demonstrating that basicity and donor ability of the incoming nucleophile must be of secondary importance in determining the rate of conversion.[30,36] This behavior is well-known and completely consistent with previous studies of the associative substitution reactions of late transition metal centers.[28,29,37] If the rate determining step of this process was formation of monomer **12** from intermediate **15**, one would expect the rate of conversion to be inversely dependent on the strength of the nucleophile−Rh bond being broken in this step and, therefore, the basicity of the phosphine used to initiate the reaction. Additionally, the observation of a build-up of the concentration of **15** (or its chelated analogue) in solution would be expected. If the slow step in this reaction scheme was the attack of the pendant phosphine arm of **15** on the sterically crowded Rh(I) metal center one would again expect to see an observable amount of intermediate **15**. The data also agree well with the relatively small value for the enthalpy of activation and indicate the importance of the bond formation in the transition state of the reaction, which is directly affected by the steric bulk of the incoming ligand and its ability to access the transition metal centers of complex **8**. Additionally, the bidentate phosphines (BDPO and **7**) can be compared to evaluate the role of chelation when **7** is used to catalyze the conversion. Specifically, when one considers the structural similarities and differences of BDPO and **7**, they can be compared to gain insight into the importance of the hemilabile nature of ligand **7** in the conversion of **8** into **12**. Because the rate of reaction catalyzed by **7** is only slightly faster than that of the BDPO-catalyzed reaction (1.25 times larger rate constant, Table 2), it is concluded that the hemilabile nature of **7** and the presence of an arene ring capable of binding to the metal play a minor role, if any, in the phosphine-catalyzed conversion of **8** into **12**.

Conclusions

In summary, we report binuclear and mononuclear rhodium macrocycles based on the unsymmetric 1,4-bis-(2-diphenylphosphinoethoxy)naphthalene ligand that have been fully characterized by various means including multidimensional NMR and X-ray crystallography. The use of a naphthalene aromatic core in the title ligand and its ability to facilitate different binding modes to the rhodium(I) metal center via ring slippage have provided the first mechanistic insight into the process by which this class of kinetically stable binuclear complexes converts to the corresponding mononuclear complexes. Specifically, based on kinetic studies of this process, we propose an associative mechanism for this conversion catalyzed by the addition of phosphine ligands. These studies demonstrate the importance of the hemilabile nature of the ligands used in the Weak-Link Approach and the significance of the careful control of reaction conditions, including stiochiometry, for the synthesis and isolation of the desired metastable binuclear intermediate structures.

Experimental Section

General Methods. Unless otherwise noted, all reactions and manipulations were carried out under a nitrogen atmosphere using standard Schlenk techniques. Diethyl ether and tetrahydrofuran (THF) were dried and distilled over sodium and benzophenone. Acetonitrile, methylene chloride, and pentane were dried and distilled over calcium hydride. $[Rh(Cl)(COE)_2]_2$ (COE = cyclooctene) was prepared according to a literature method using $RhCl_3$ and COE in 2-propanol.[38] Commercial purity carbon monoxide was purchased from Matheson Gas and passed through a 15-cm column of Drierite before use. All other chemicals were purchased from common commercial sources (Aldrich, TCI, Acros, and Cambridge Isotopes) and used as received. The purity of the phosphine reagents utilized in the kinetic studies was verified by $^{31}P\{^1H\}$ NMR spectroscopy prior to their use. One-dimensional NMR spectra were recorded on a Varian 300-MHz spectrometer. Two-dimensional and $^{13}C\{^1H\}$ NMR (125 MHz) spectra

(35) Hudson, H. R. In *The Chemistry of Organophosphorus Compounds*; Hartley, F. R., Ed.; Wiley & Sons: New York, 1990; Vol. 1, pp 473−488.

(36) (a) Morris, D. E.; Basolo, F. *J. Am. Chem. Soc.* **1968**, *90*, 2531−2535. (b) Schuster-Woldan, H. G.; Basolo, F. *J. Am. Chem. Soc.* **1966**, *88*, 1657−1663. (c) Thorsteinson, E. M.; Basolo, F. *J. Am. Chem. Soc.* **1966**, *88*, 3929−3936.

(37) (a) Howell, J. A. S.; Dixon, D. T.; Kola, J. C.; Ashford, N. F. *J. Organomet. Chem.* **1985**, *294*, C1−C4. (b) Butler, I. S.; Ismail, A. A. *Inorg. Chem.* **1986**, *25*, 3910−3914.

(38) *Reagents for Transition Metal Complex and Organometallic Synthesis*; Angelici, R. J., Ed.; John Wiley & Sons: New York, 1990; Vol. 28.

of **8** and **12** were recorded on a Varian 500-MHz spectrometer. ^{1}H NMR signals are reported relative to residual proton resonances in deuterated solvents. ^{31}P{^{1}H} NMR spectra were recorded at 121 MHz and referenced versus an 85% H_3PO_4 external standard. ^{13}C{^{1}H} NMR spectra were recorded at 75 MHz. All chemical shifts are reported in ppm and coupling constants in Hz. Elemental analyses were performed by QTI, Whitehouse, NJ (www.qtionline.com). Combustion analysis was not used for compounds **9**, **10**, **11**, and **13** due to the relative lability of the acetonitrile and carbon monoxide ligands under combustion conditions. Electrochemical measurements were carried out with a PINE AFRDE5 bipotentiostat/glavanostat using a Au electrode with a Pt mesh counter electrode and a silver wire quasireference electrode in a 0.1 M *n*-Bu_4NPF_6/CH_2Cl_2 solution. Electrochemical data were referenced using the Fc/Fc$^+$ (Fc = (η^5-C_5H_5)Fe (η^5-C_5H_5)) redox couple as an internal standard.

Synthesis of 1,4-Di(2-chloroethoxy)naphthalene (6). A mixture of 1,4-dihydroxynaphthalene (2.0 g, 12.49 mmol), 1,2-dichloroethane (25 mL, 0.32 mol), potassium carbonate (8.0 g, 57.89 mmol), and 18-crown-6 (0.5 g, 1.89 mmol) in acetone (25 mL) was heated at reflux with vigorous stirring for 24 h. The mixture was allowed to cool to room temperature and diluted with dichloromethane (~300 mL). The reaction mixture was vacuum filtered through a Celite and silica gel pad and evaporated to dryness. The crude product was titrated with ethanol, which gave analytically pure product (2.9 g, 82%). Mp 121−123 °C. ^{1}H NMR ($CDCl_3$): δ 3.95 (t, J_{H-H} = 6.0, 4H, CH_2-Cl), 4.37 (t, J_{H-H} = 6.0, 4H, CH_2O), 6.71 (s, 2H, $C_{10}H_6$), 7.55 (m, 2H, $C_{10}H_6$), 8.27 (m, 2H, $C_{10}H_6$). ^{13}C{^{1}H} NMR (CD_2Cl_2): δ 42.39 (s, *C*H_2Cl), 68.98 (s, O*C*H_2), 105.11 (s, $C_{2/3}$), 122.05 (s, $C_{9/10}$), 126.48 (s, $C_{5/8}$), 126.77 (s, $C_{6/7}$), 148.82 (s, $C_{1/4}$). HRMS (EI, *m*/*z*): 284.03715 (calcd for $C_{14}H_{14}Cl_2O_2$ 284.03708). Anal. Calcd for $C_{14}H_{14}Cl_2O_2$: C, 58.97; H, 4.95. Found: C, 58.72; H, 4.97.

Synthesis of 1,4-Bis(2-(diphenylphosphino)ethoxy)-naphthalene (7). $KPPh_2$ (0.5 M, 4.4 mL, 2.20 mmol) in 50 mL of THF was added dropwise to a THF (100 mL) solution of **6** (0.35 g, 1.07 mmol) under ice-bath cooling for 1 h and the mixture was stirred overnight at room temperature. After the evaporation of solvent, the organic materials were extracted with dichloromethane from water. Combined organic phases were dried using anhydrous $MgSO_4$ and then in vacuo. The white solid was suspended in EtOH (30 mL) and isolated via cannula filtration. The resulting solid was dried under vacuum overnight (0.55 g, 88%). Mp 145−146 °C. ^{1}H NMR (CD_2Cl_2): δ 2.71 (t, J_{H-H} = 7.2, 4H, CH_2PPh$_2$), 4.25 (dt (pseudoquartet), J_{H-H} = 7.2, J_{P-H} = 9.6, 4H, CH_2O), 6.57 (s, 2H, $C_{10}H_6$), 7.39 (m, 12H, P(C_6H_5)$_2$ + $C_{10}H_6$), 7.51 (m, 10H, P(C_6H_5)$_2$), 7.89 (m, 2H, $C_{10}H_6$). ^{13}C{^{1}H} NMR (CD_2Cl_2): δ 28.94 (d, J_{C-P} = 13.1, *C*H_2PPh$_2$), 66.58 (d, J_{C-P} = 23.9, *C*H_2O), 104.77 (s, $C_{2/3}$), 122.28 (s, $C_{5/8}$), 126.16 (s, $C_{6/7}$), 126.80 (s, $C_{9/10}$), 129.07 (d, J_{C-P} = 6.5, C_m−P), 129.26 (s, C_p−P), 133.26 (d, J_{C-P} = 19.1, C_o−P), 138.96 (d, J_{C-P} = 12.8, C_i−P), 148.95 (s, $C_{1/4}$). ^{31}P{^{1}H} NMR(CD_2Cl_2): δ −21.29 (s). HRMS (EI, *m*/*z*): 584.20344 (calcd for $C_{38}H_{34}O_2P_2$ 584.20340). Anal. Calcd for $C_{38}H_{34}O_2P_2$: C, 78.06; H, 5.87; P, 10.60. Found: C, 77.85; H, 5.79; P, 10.37.

Synthesis of [(μ^2,η^1:η^4:η^1-(1,4-Bis(2-(diphenylphosphino)-ethoxy)naphthalene))$_2$Rh$_2$] [BF$_4$]$_2$ (8). In a glovebox [Rh(Cl)(COE)$_2$]$_2$ (40 mg, 1.13 × 10^{-4} mol) and $AgBF_4$ (22 mg, 1.13 × 10^{-4} mol) were reacted in 3 mL of CH_2Cl_2 for 30 min. The resulting reaction mixture was filtered through Celite, and the filtrate was diluted with 125 mL of THF. To this, a solution of **7** (66 mg, 1.129 × 10^{-4} mol) in 125 mL of THF was added dropwise at −78 °C over 2 h and then warmed to room temperature over 1 h. The solvent was removed under vacuum to yield an orange-red powder. The solid was dissolved in a small amount of CH_2Cl_2 and precipitated with pentane. The resulting orange-red solid was collected over Celite and redissolved in CH_2Cl_2. A few drops of CH_3CN were added to this solution and stirred for 20 min at room temperature. The solvent was pumped off in vacuo and the resulting solid was dried overnight at 55 °C under vacuum (80 mg, 92%). Dec pt 184 °C. ^{1}H NMR (CD_2Cl_2): δ 1.88 (m, 2H, CH_2PPh$_2$), 2.11 (m, 2H, CH_2PPh$_2$), 2.43 (m, 2H, CH_2PPh$_2$), 2.58 (m, 2H, CH_2PPh$_2$), 3.86 (m, 2H, CH_2O), 4.00 (m, 2H, CH_2O), 4.62 (m, 2H, CH_2O), 5.35 (m, 2H, CH_2O), 6.22 (m, 4H, P(C_6H_5)$_2$), 6.62 (m, 4H, P(C_6H_5)$_2$ + $C_{10}H_6$), 6.87 (m, 14H, P(C_6H_5)$_2$), 7.07 (m, 2H, P(C_6H_5)$_2$), 7.19 (m, 4H, P(C_6H_5)$_2$), 7.39 (m, 8H, P(C_6H_5)$_2$ + $C_{10}H_6$), 7.67 (m, 2H, P(C_6H_5)$_2$), 7.78 (m, 6H, P(C_6H_5)$_2$ + $C_{10}H_6$), 8.15 (m, 4H, P(C_6H_5)$_2$), 8.34 (d, J_{H-H} = 8.4, 2H, $C_{10}H_6$), 8.42 (d, J_{H-H} = 6.6, 2H, $C_{10}H_6$). ^{13}C{^{1}H} NMR (125.641 MHz, CD_2Cl_2): δ 26.31 (d, J_{C-P} = 31.4, *C*H_2PPh$_2$), 30.46 (d, J_{C-P} = 26.8, *C*H_2PPh$_2$), 66.41 (s, *C*H_2O), 69.40 (d, J_{C-P} = 16.5, *C*H_2O), 78.49 (s, $C_{2/3}$), 89.15 (s, $C_{2/3}$), 115.75 (s, $C_{1/4}$), 117.09 (dd, J_{C-P} = 7.5, J_{C-Rh} = 2.5, $C_{1/4}$), 119.88 (s, $C_{5/8}$), 120.35 (s, $C_{5/8}$), 121.24 (s, $C_{9/10}$), 127.90 (s, $C_{9/10}$), 128.13 (m, P(C_6H_5)$_2$), 128.30 (m, P(C_6H_5)$_2$), 128.56 (m, P(C_6H_5)$_2$), 128.89 (s, $C_{6/7}$), 129.29 (s, $C_{6/7}$), 129.63 (m, P(C_6H_5)$_2$), 130.44 (m, P(C_6H_5)$_2$), 130.59 (m, P(C_6H_5)$_2$), 130.91 (m, P(C_6H_5)$_2$), 131.05 (m, P(C_6H_5)$_2$), 131.36 (m, P(C_6H_5)$_2$), 131.60 (m, P(C_6H_5)$_2$), 131.72 (m, P(C_6H_5)$_2$), 132.50 (m, P(C_6H_5)$_2$), 132.52 (m, P(C_6H_5)$_2$), 133.20 (m, P(C_6H_5)$_2$), 134.55 (m, P(C_6H_5)$_2$), 137.15 (m, P(C_6H_5)$_2$). ^{31}P{^{1}H} NMR (CD_2Cl_2): δ 25.66 (dd, J_{P-P} = 40, J_{Rh-P} = 205), 34.91 (dd, J_{P-P} = 40, J_{Rh-P} = 216). MS (ESI, *m*/*z*): [M − BF_4^-]$^+$ 1461.7 (calcd for $C_{76}H_{68}BF_4O_4P_4Rh_2^+$ 1461.9), [M − 2BF_4^-]$^{2+}$ 687.5 (calcd for $C_{76}H_{68}O_4P_4Rh_2^{2+}$ 687.5). Anal. Calcd for $C_{76}H_{68}B_2F_8O_4P_4Rh_2$: C, 58.91; H, 4.43; P, 8.00. Found: C, 58.24; H, 4.48; P, 7.84.

Synthesis of [(μ^2-1,4-Bis(2-(diphenylphosphino)ethoxy)-naphthalene)$_2$Rh$_2$(CD$_3$CN)$_4$][BF$_4$]$_2$ (9). Three drops of acetonitrile-d_3 was added to a CD_2Cl_2 solution of **8** (10 mg in 0.5 mL). The solution color changed from deep-red to yellow indicating the formation of **9**. ^{1}H NMR (CD_2Cl_2): δ 2.97 (m, 8H, CH_2PPh$_2$), 4.58 (m, 8H, CH_2O), 6.66 (m, 4H, $C_{10}H_6$), 6.86−8.14 (m, 48H, P(C_6H_5)$_2$ + $C_{10}H_6$). ^{31}P{^{1}H} NMR (CD_2Cl_2): δ 39.1 (d, J_{Rh-P} = 172.8), 37.3 (d, J_{Rh-P} = 172.8), 24.4 (d, J_{Rh-P} = 130.6), 24.1 (d, J_{Rh-P} = 130.6). MS (ESI, *m*/*z*): [M − 4CD_3-CN − BF_4^-]$^+$ 1461.2 (calcd for $C_{76}H_{68}BF_4O_4P_4Rh_2^+$ 1461.9), [M − 4CD_3CN − 2BF_4^-]$^{2+}$ 687.4 (calcd for $C_{76}H_{68}O_4P_4Rh_2^{2+}$ 687.5).

Synthesis of [(μ^2-1,4-Bis(2-(diphenylphosphino)ethoxy)-naphthalene)$_2$Rh$_2$(CO)$_6$][BF$_4$]$_2$ (10). A CD_2Cl_2 solution of **8** (10 mg in 0.5 mL) was charged with CO gas for 3 h at room temperature. The resulting solution was agitated overnight with a mechanical shaker. The solution changed from deep-red to a pale-yellow color with a white precipitate. ^{31}P{^{1}H} NMR spectroscopic data of the supernatant solution and the redissolved precipitate show the formation of tricarbonylrhodium(I) complex **10** in a quantitative yield. ^{1}H NMR (CD_2Cl_2): δ 3.22 (m(b), 8H, CH_2PPh$_2$), 4.50 (m(b), 8H, CH_2O), 6.54 (s(b), 4H, $C_{10}H_6$), 7.26 (m, 4H, $C_{10}H_6$), 7.51−7.71 (m, 44H, P(C_6H_5)$_2$ + $C_{10}H_6$). ^{31}P{^{1}H} NMR (CD_2Cl_2): δ 26.81 (d, J_{Rh-P} = 90). MS (ESI, *m*/*z*): [M − 6CO − BF_4^-]$^+$ 1461.6 (calcd for $C_{76}H_{68}$-$BF_4O_4P_4Rh_2^+$ 1461.9), [M − 6CO − 2BF_4^-]$^{2+}$ 687.4 (calcd for $C_{76}H_{68}O_4P_4Rh_2^{2+}$ 687.5). FTIR (CD_2Cl_2): ν_{CO} 2013 (s), 2093 (s) cm^{-1}.

Synthesis of [(μ^2-1,4-Bis(2-(diphenylphosphino)ethoxy)-naphthalene)$_2$(CO)$_2$Rh$_2$ (CD$_3$CN)$_2$][BF$_4$]$_2$ (11). The precipitate of **10** was collected by filtration of the CD_2Cl_2 suspension (vide supra) through Celite. The solid was then redissolved with CD_3CN and evolution of CO gas was observed. NMR spectroscopy shows the quantitative formation of the *trans*-CO-Rh(I)-NCCD$_3$ complex, **11**. ^{1}H NMR (CD_3CN): δ 3.21 (m, 8H, CH_2PPh$_2$), 4.44 (m, 8H, CH_2O), 6.42 (s, 4H, $C_{10}H_6$), 7.33 (m, 4H, $C_{10}H_6$), 7.50 (m, 24H, P(C_6H_5)$_2$), 7.64 (m, 4H, $C_{10}H_6$), 7.71 (m, 16H, P(C_6H_5)$_2$). ^{31}P{^{1}H} NMR (CD_3CN): δ 27.52 (d, J_{Rh-P} = 118). MS (ESI, *m*/*z*): [M − BF_4^-]$^+$ 1605.7 (calcd for $C_{82}H_{68}D_6BF_4N_2O_6P_4Rh_2^+$ 1606.0), [M − 2BF_4^-]$^{2+}$ 759.6 (calcd for $C_{82}H_{68}D_6N_2O_6P_4Rh_2^{2+}$ 759.5), [M − 2CO − 2CD_3CN − 2BF_4^-]$^{2+}$ 687.8 (calcd $C_{80}H_{68}D_6N_2O_4P_4Rh_2^{2+}$ 687.5). FTIR (CD_3-CN): ν_{CO} 1943 (s) cm^{-1}.

Synthesis of [(η^1:η^4:η^1-1,4-Bis(2-(diphenylphosphino)-ethoxy)naphthalene)Rh][BF$_4$] (12). Complex **8** (10 mg, 6.46

Table 3. Crystallographic Data for 8, 9 (*cis*-, *anti*-), 11, and 12

entry	**8**	**9** (*cis*-, *anti*-)	**11**	**12**
formula	$C_{77.25}H_{68}B_2F_8O_{4.25}P_4Rh_2Cl_{1.5}$	$C_{84}H_{80}B_2F_8N_4O_4P_4Rh_2\cdot 2(CH_2Cl_2)\cdot 2(H_2O)$	$C_{82}H_{74}B_2F_8N_2O_6P_4Rh_2\cdot 2(CH_3CN)$	$C_{38}H_{34}BF_4O_2P_2Rh$
fw	1620.81	1918.72	1768.86	774.31
color, habit	red, block	yellow, block	yellow, block	red, block
cryst dimens (mm^3)	0.45 × 0.15 × 0.07	0.10 × 0.10 × 0.10	0.20 × 0.18 × 0.12	0.30 × 0.30 × 0.20
space group	*Cc*	$P\bar{1}$	$P2_1/c$	$P2_1$
cryst syst	monoclinic	triclinic	monoclinic	monoclinic
a, Å	22.986(3)	10.693(2)	11.3786(6)	10.3886(5)
b, Å	30.121(4)	12.056(2)	19.4572(10)	13.9509(6)
c, Å	16.062(2)	18.979(3)	18.9976(10)	11.8759(5)
α, deg	90	84.261(3)	90	90
β, deg	129.574(2)	89.892(3)	99.8450(10)	103.9520(10)
γ, deg	90	83.049(3)	90	90
V, $Å^3$	8572(2)	2416.3(8)	4144.0(4)	1670.40(13)
Z	4	1	2	2
D_{calcd}, g cm^{-3}	1.256	1.319	1.418	1.539
radiation (*λ*, D)	Mo Kα (0.71073)	Mo Kα (0.71073)	Mo Kα (0.71073)	Mo Kα (0.71073)
F(000)	3292	980	1808	788
2*θ* range, deg	2.66−56.54	2.16−57.6	3.02−56.58	4.68−56.48
μ, cm^{-1}	5.65 (Mo Kα)	5.80 (Mo Kα)	5.48 (Mo Kα)	6.64 (Mo Kα)
range of trans factors	0.9058−1.00	0.63−1.00	0.8983−0.9371	0.8257−0.8787
T, K	153	150(2)	183(2)	173(2)
scan method	*ω*	*ω*	*ω*	*ω*
abs cor	empirical from SADABS			
no. of measd reflns	39692	14897	21022	7128
no. of indep reflns	25467	10565	8984	5505
refinement method	full-matrix least-squares on F^2			
GOF on F^2	1.09	1.150	1.021	1.031
final *R* indices[a] ($I > 2\sigma(I)$)	R1 = 0.0483, wR2 = 0.1310	R1 = 0.0786, wR2 = 0.1911	R1 = 0.0454, wR2 = 0.1106	R1 = 0.0201, wR2 = 0.0534
R indices (all data)	R1 = 0.0558, wR2 = 0.1386	R1 = 0.0947, wR2 = 0.2014	R1 = 0.0735, wR2 = 0.1248	R1 = 0.0208, wR2 = 0.0536

[a] $R1 = \sum||F_o| - |F_c||/\sum|F_o|$, $wR2 = [\sum(w(F_o^2 - F_c^2)^2)/\sum w(F_o^2)^2]^{1/2}$, $w = 1/\sigma^2(F^2)$.

× 10^{-6} mol) was dissolved in 0.5 mL of CD_2Cl_2 to which ligand **7** was added (2 mg, 3.23 × 10^{-6} mol). The sealed NMR tube was warmed to 50 °C for 48 h, which quantitatively gave monomeric Rh(I) complex and free ligand without any decomposition as determined by NMR spectroscopy. Repeated precipitation (3 times) of complex **12** from CH_2Cl_2 with diethyl ether afforded analytically pure monomeric complex (9 mg, 90%). Dec pt 270 °C. ^{1}H NMR (CD_2Cl_2): *δ* 1.98 (m, 2H, CH_2-PPh_2), 2.08 (m, 2H, CH_2PPh_2), 4.30 (m, 2H, CH_2O), 4.47 (m, 2H, CH_2O), 6.64 (m, 4H, P(C_6H_5)$_2$), 6.96 (s, 2H, $C_{10}H_6$), 7.00 (m, 4H, P(C_6H_5)$_2$), 7.15 (m, 10H, P(C_6H_5)$_2$), 7.25 (m, 2H, P(C_6H_5)$_2$), 7.73 (m, 2H, $C_{10}H_6$), 7.93 (m, 2H, $C_{10}H_6$). ^{13}C{^{1}H} NMR (125.641 MHz, CD_2Cl_2): *δ* 24.88 (m, CH_2PPh_2), 69.03 (s, CH_2O), 87.77 (d, J_{C-Rh} = 3.4, $C_{2/3}$), 116.62 (d, J_{C-Rh} = 3.3, $C_{1/4}$), 120.84 (s, $C_{5/8}$), 122.09 (s, $C_{9/10}$), 128.72 (m, C_m−P), 128.98 (m, C_m−P), 130.14 (s, $C_{6/7}$), 130.35 (m, C_i−P), 130.74 (m, C_i−P), 131.06 (s, C_p−P), 131.33 (s, C_p−P), 133.38 (m, C_o−P), 134.03 (m, C_o−P). ^{31}P{^{1}H} NMR (CD_2Cl_2): *δ* 27.29 (d, J_{Rh-P} = 202). MS (ESI, *m*/*z*): $[M - BF_4^-]^+$ 687.3 (calcd for $C_{38}H_{34}O_2P_2Rh^+$ 687.5). Anal. Calcd for $C_{38}H_{34}BF_4O_2P_2Rh$: C, 58.91; H, 4.43; P, 8.00. Found: C, 58.85; H, 4.29; P, 7.75. $E_{1/2}$ (CH_2Cl_2, 0.1 M [(*n*-Bu)$_4$N][PF_6]): 660 mV (vs Fc/Fc^+).

Synthesis of [(*η*^{1}:*η*^{1}-1,4-Bis(2-(diphenylphosphino)-ethoxy)naphthalene)(CO)Rh(CH_3CN)][BF_4] (13). Three drops of CH_3CN was added to a CD_2Cl_2 solution of **12** (10 mg in 0.5 mL), which was then charged with CO (1 atm) for 2 h at room temperature. The resulting NMR solution was shaken overnight, which gave a monomeric *trans*-CO-Rh(I)-$NCCD_3$ complex quantitatively as determined by NMR spectroscopy. ^{1}H NMR (CD_2Cl_2): *δ* 2.90 (m, 2H, CH_2PPh_2), 3.14 (m, 2H, CH_2-PPh_2), 4.42 (m, 4H, CH_2O), 6.40 (s, 2H, $C_{10}H_6$), 7.18−7.79 (m, 24H, P(C_6H_5)$_2$ + $C_{10}H_6$). ^{31}P{^{1}H} NMR(CD_2Cl_2): *δ* 23.56 (d, J_{Rh-P} = 117). MS (ESI, *m*/*z*): $[M - BF_4^-]^+$ 756.3 (calcd for $C_{41}H_{37}NO_3P_2Rh$ 756.6), $[M - CH_3CN - BF_4^-]^+$ 715.3 (calcd for $C_{39}H_{34}O_3P_2Rh^+$ 715.5), $[M - CO - CH_3CN - BF_4^-]^+$ 687.4 (calcd for $C_{38}H_{34}O_2P_2Rh^+$ 687.5).

Kinetic NMR Experiments. Monophosphine (0.2 equiv, 43 *μ*L, 2 × 10^{-2} M in CD_2Cl_2) or 0.1 equiv of diphosphine (43 *μ*L, 1 × 10^{-2} M in CD_2Cl_2) was added to a solution of **8** (7 mg, 4.5 × 10^{-6} mol) in 0.5 mL of 1 × 10^{-3} M decane in CD_2Cl_2 in an air-free NMR tube. The mixture was placed in an NMR spectrometer, and the temperature was maintained at 40 °C over the duration of the experiment. The ^{1}H NMR spectra were recorded periodically (every 5−20 min; depending on the temperature of experiment). Comparison of the relative integrations of decane to **8** provided conversion data of **8** to **12**. The data were fit to rate laws for zero-, first-, and second-order kinetics. The first-order plots (ln[**8**] vs time) showed a linear relationship, and the k_{obsd} were determined from the slope of this line by the linear least-squares method. The correlation coefficient of the least-squares line (R^2 > 0.997) was very good. Furthermore, to ensure statistical accuracy, the variation of macrocycle concentration vs time was fit directly to the nonlinear rate law using nonlinear least-squares analysis. The variable-temperature kinetics were performed in an identical manner at 30, 35, 45, and 50 °C. All reactions proceed to completion to give **12** and free nucleophile as confirmed by ^{1}H and ^{31}P{^{1}H} NMR spectroscopies.

X-ray Crystallography. A suitable X-ray quality crystal of **8** coated with Paratone was mounted on a Bruker SMART-1000 diffractometer equipped with a graphite-monochromated Mo Kα (*λ* = 0.71073) radiation source and a CCD detector. Data collection was performed with a detector distance of 5 cm. The raw data collected were processed to produce conventional intensity data by the program SAINT. The intensity data were corrected for Lorentz and polarization effects. Absorption correction was also applied using the SADABS empirical method. The structure was solved by direct methods provided by the program package SIRS92. Unless otherwise noted, all the non-hydrogen atoms were refined anisotropically. Hydrogen atom positions were calculated and included in the final cycle of refinement. Suitable crystals of **9** (*cis*-, *anti*-), **11**,

and **12** were selected and glued to a thin glass fiber using epoxy. The structures were solved using direct methods for **11** and **12** and the Patterson function for **9** (*cis*-, *anti*-). Non-hydrogen atoms were located by Fourier synthesis and were refined anisotropically. Hydrogen atoms were added at calculated positions and treated as isotropic contributions with thermal parameters defined as 1.2 or 1.5 times that of the parent atom. The systematic absences in diffraction data of **11** and **12** were consistent with the reported space groups. The *E*-statistics suggested a centrosymmetric space group for **9** (*cis*-, *anti*-). The solvent molecules in the structure of **9** (*cis*-, *anti*-) are disordered. The program SQUEEZE[39] was used to treat the solvent molecules. Corrections of the X-ray data for **9** (*cis*-, *anti*-) by SQUEEZE (113 electron/cell) are close to the required value (104 electron/cell) for the formula above. The correct absolute structure was unambiguously determined; Flack parameter = 0.14(3) and 0.007(16) respectively for **8** and **12**. All software and sources of scattering factors are contained in the SHELXTL program library (version 5.10, G. Sheldrick, Bruker-AXS, Madison, WI.). Crystallographic data for **8**, **9** (*cis*-, *anti*-), **11**, and **12** are summarized in Table 3.

(39) Van der Sluis, P.; Spek, A. L. *Acta Crystallogr.* **1990**, *A46*, 194−201.

Acknowledgment. C.A.M. acknowledges the NSF (CHE-0071885/001) and AFOSR (F49620-00-1-0230) for support of this research. B.J.H. acknowledges Sigma Xi, the Link Foundation, and NSF/NSEC (EEC-0118025) for fellowship support. Y.-M.J. acknowledges the Korea Research Foundation (KRF-99-D031) for postdoctoral fellowship support. Professors J. B. Lambert and Fred Basolo are gratefully acknowledged for helpful discussions.

Supporting Information Available: The COSY and HMQC spectra of complex **8** and the HMQC spectrum of **12**; images of the reaction described in footnote 7b and the $^{31}P\{^{1}H\}$ NMR spectrum of the crude reaction mixture. This material is available free of charge via the Internet at http://pubs.acs.org.

OM020739C